A Theoretical Study of the Properties and Reactivities of Ketene, Thioketene, and Selenoketene

Ngai Ling Ma[a] and Ming Wah Wong*[a]

Keywords: Calculations, ab initio / Reaction mechanisms / Ketenes / Cumulenes / Cycloaddition reactions / Nucleophilic addition / Electrophilic addition

The properties and reactivities of ketene, thioketene, and selenoketene were studied using the G2(MP2) level of theory. Calculated structures, vibrational frequencies, dipole moments, NMR chemical shifts, and charge distributions strongly suggest that thioketene and selenoketene are best represented by the neutral cumulenic form. Four prototype reactions were examined: ketene-ynol rearrangement, electrophilic and nucleophilic addition, and [2+2] cycloaddition. Thioketene and selenoketene were found to be more reactive than ketene in all reactions. In terms of chemistry, thioketene resembles selenoketene more than ketene. The variation of reactivity can readily be explained in terms of strain energy, electronegativity, and molecular orbital arguments.

Introduction

Ketene (RR′C=C=X, where X = O), arguably one of the most versatile organic synthetic intermediates, was first prepared in 1905.[1] The sulfur and selenium analogs of ketene, namely thioketene and selenoketene (where X = S and Se, respectively), were only prepared more recently. In biological systems, the general importance of organoselenium compounds has long been recognized.[2] Recently, it has been suggested that thioketene could be involved in cell damage processes.[3] Even though thioketene and selenoketene have been characterized spectroscopically,[4,5] some physical properties as well as their intrinsic reactivities are not known, as these species dimerize spontaneously.[6,7]

We report, here, an ab initio molecular-orbital study on the properties and reactivities of ketene, thioketene, and selenoketene ($H_2C=C=X$, where X = O, S, and Se). Firstly, we will examine the structural, spectroscopic, and thermochemical properties of these ketenes. Then, we will report our results on four prototype reactions of ketene: ketene-ynol rearrangement, addition reactions with electrophiles and nucleophiles, and [2+2] cycloaddition with ethene. For ketene itself, these reactions are well studied both theoretically and experimentally.[1] Some information is available for thioketene[8] but virtually no information is available for selenoketene. By studying these processes at a uniform level of theory, the intrinsic reactivities of these ketenes may be compared.

Computational Methods

Standard ab initio calculations were performed using the Gaussian 94[9] and 98[10] series of programs. Unless otherwise stated, all energies reported in this paper are at the G2(MP2) level of theory.[11] In brief, G2(MP2) is a composite procedure which aims to provide an accurate approximation to the high level of theory at QCISD(T)/6-311+G(3df,2p)//MP2(FU)/6-31G(d), with the incorporation of zero-point energy [calculated from HF/6-31G(d) frequencies, scaled by 0.8929] and higher level corrections. This level of theory is usually within ±3 kcal mol^{-1} (approximately 12 kJ mol^{-1}) of the accurate experimental values. The optimized geometries [MP2(FU)/6-31G(d)] of all species studied in this paper are shown in Figure 1, and are labelled from **1** to **19**. In order to distinguish between the same structure with different substituents (O, S, or Se), the number will be prefixed by the atomic symbol of the substituent. For example, ketene, thioketene, and selenoketene are denoted as **O1**, **S1**, and **Se1**, respectively. The G2(MP2) electronic energies (E_0) of all these species are given in Table 1.

We have also investigated the effect of core size on the energetics of the selenium containing systems, this topic has recently attracted some attention.[12,13] Specifically, we compare calculated ionization energies (*IE*s) and reaction energies using three different approaches: (1) a full core (i.e. include all electrons), (2) a frozen core excluding the 3d electrons [which corresponds to the G2(d) level of theory],[13] and (3) a frozen core including the 3d electrons (i.e. the default frozen core size). We found that both the *IE* and the reaction energies are not sensitive to the size of the core. Given the substantial resource saving in using the frozen core approximation in correlation calculations, we continue to apply such an approximation here.

Results and Discussion

Properties of Ketene, Thioketene and Selenoketene

We have investigated several fundamental physical properties of the ketenes, including geometries, vibrational fre-

[a] Department of Chemistry, National University of Singapore, Kent Ridge, Singapore 119260
Fax: (internat.) + 65/7791691
E-mail: chmwmw@nus.edu.sg

  1434−193X/00/0408−1411 $ 17.50+.50/0

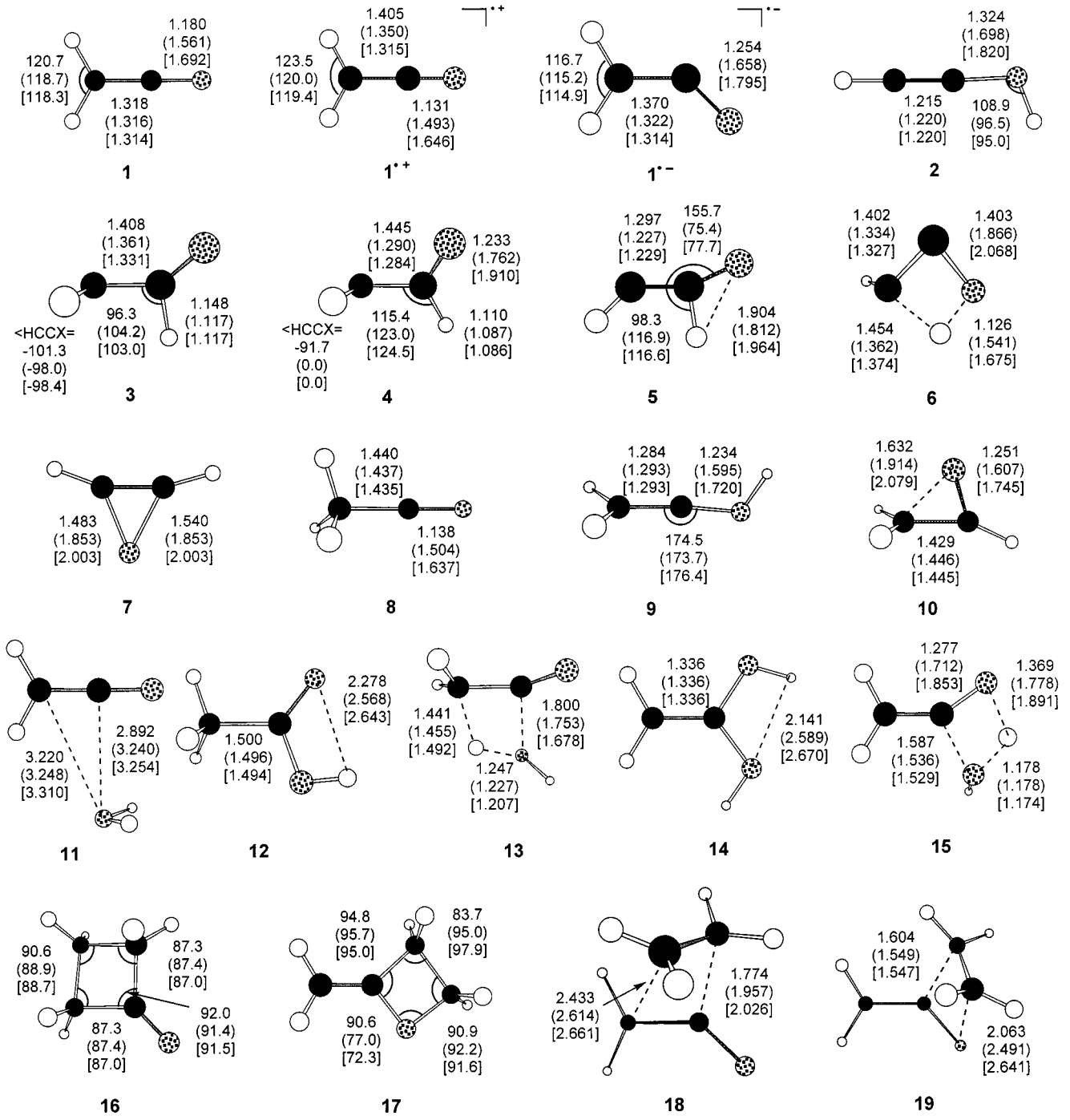

Figure 1. Optimized geometries [MP2(FU)/6-31G(d)] for ketenes and related species; structural parameters are given in parentheses for thioketene and in bracket for selenoketene (bond lengths in Å and angles in degrees)

quencies, ^{13}C-NMR chemical shifts, dipole moments, heats of formation, ionization energies, and proton and electron affinities, and the results are summarized in Table 2.

The structures of ketene, thioketene and selenoketene are known experimentally.[4,5] Our calculated structures at the MP2(FU)/6-31G(d) level are in good general agreement with the reported experimental structures, with a maximum error in bond length and angle of 0.02 Å and 1.4°, respectively, but slightly inferior to those reported by Leszczynski[4] at the MP2/TZP level. At our best level of theory, QCISD/6-311+G(2df,p), the maximum errors in bond length and angle reduce to only 0.006 Å and 0.9°, respectively. The trends of decrease in r_{CC} and $\angle_{HCH}$, and increase in r_{CH} length when oxygen is substituted by the heavier atom are readily reproduced.

Experimental vibrational frequencies of these species have been reported.[5,7] We have recently found that vibrational frequencies calculated at the B3-LYP/6-31G(d) level are more reliable than those obtained at the computationally more expensive MP2 and QCISD methods with the same basis set.[14,15] Using the recommended scaling factor of 0.9613[14,15] for B3-LYP/6-31G(d) frequencies, the root-

Table 1. G2(MP2) E_0 electronic energies (Hartrees) of various species related to $H_2C{=}C{=}X$ (X = O, S, and Se)

Species[a]	X = O	X = S	X = Se
1	–152.36550	–474.95094	–2477.18696
2	–152.30986	–474.92568	–2477.16640
3	–152.24199	–474.83994	–2477.08657
4	–152.23759	–474.84789	–2477.10457
5	–152.22642	–474.84967	–2477.09939
6	–152.15793	–474.80326	–2477.05898
7	–152.24428	–474.89703	–2477.14960
8	–152.67792	–475.27222	–2477.50873
9	–152.61000	–475.23083	–2477.47187
10	–152.58987	–475.22780	–2477.47434
11	–228.69809	–551.28309	–2553.51842
12	–228.74759	–551.32401	–2553.56195
13	–228.62848	–551.19796	–2553.43486
14	–228.70354	–551.29603	–2553.53913
15	–228.63273	–551.23182	–2553.47539
16	–230.81343	–553.39881	–2555.63754
17	–230.78440	–553.40214	–2555.64590
18	–230.73358	–553.32332	–2555.56367
19	–230.69488	–553.31313	–2555.56245
$\mathbf{1}^{\bullet+}$[b]	–152.01335	–474.62228	–2476.86571
$\mathbf{1}^{\bullet+}$[c]	–152.00358	–474.61953	–2476.86527
$\mathbf{1}^{\bullet-}$[d]	–152.35119	–474.96399	–2477.21012
$\mathbf{1}^{\bullet-}$[e]	–152.31091	–474.94907	–2477.19496
(**2**–H)$^-$[f]	–151.78209	–474.39887	–2476.64655

[a] G2(MP2) energies of other species related to the reactions of the ketenes: –37.78389 (C), –0.50000 (H), –74.97868 (O), –397.64699 (S), –2399.91929 (Se), –76.33000 (H_2O), –78.41428 (C_2H_4) hartrees. – [b] Ketene radical cation, with the geometry of the neutral ketene. – [c] Ketene radical cation, fully optimized. – [d] Ketene radical anion, with the geometry of the neutral ketene. – [e] Ketene radical anion, fully optimized. – [f] Ynolate anion.

mean-square (RMS) errors of the calculated frequencies for ketene, thioketene, and selenoketene are 13, 19, and 29 cm^{-1}, respectively. These errors are well within the expected RMS error of 34 cm^{-1} for the B3-LYP/6-31G(d) frequencies. Thus, it appears that even though no selenium compound was used in deriving the scaling factor, the recommended scaling factor is equally applicable to selenium containing compound.

The ^{13}C-NMR spectrum is a useful diagnostic tool for identification of ketene. In particular, ketene has a characteristic high field C_β shift, and this has been attributed to the high degree of negative charge on this atom. Using the QCISD/6-31G(d) geometry, we have performed MP2 GIAO (Gauge-Independent Atomic Orbital)[16] chemical shift calculations (with respect to TMS) with the 6-311G(d,p) basis set (Table 2). For ketene, the calculated ^{13}C-NMR shifts are in excellent agreement with the experimental values.[1] In particular, the characteristics high field C_β is well reproduced. We are not aware of any experimental values for thioketene and selenoketene. Here we assume that the effect of substitution at C_β on ^{13}C-NMR shift is the same for ketene and thioketene, and an estimated value for thioketene can be derived from $(Ph)_2C{=}C{=}X$, $PhMeC{=}C{=}X$, and $(Me_3Si)_2C{=}C{=}X$ (where X = O and S), and ketene itself.[1] The thus derived ^{13}C-NMR shifts for C_α and C_β of δ = 255.1 and 50.3, respectively, are in good accord with the theoretical estimates. Hence, the present calculated values for selenoketene are probably equally accurate.

The dipole moments of all three ketenes have been determined experimentally. For ketene and thioketene, the experimental dipole moments are 1.41 and 1.01 D, respectively.[4] No precise determination of the dipole moment for selenoketene is available, but an estimated value of 0.90 D has been proposed.[17] While the trend of reduction in dipole moment upon substitution with heavier atom is readily reproduced at most levels of theory, the absolute values of the dipole moment are very sensitive to the levels of theory employed. For example, we found that for ketene, the HF method tends to grossly overestimate, while MP2 tends to significantly underestimate the dipole moment. A reliable dipole moment can be obtained at the QCISD level of theory. At QCISD/6-311+G(2df,p)//QCISD/6-311+G(2df,p) level of theory, the calculated dipole for X = O, S, and Se are 1.44, 1.06, and 1.11 D, respectively. Given the good agreement (< 5%) between the experimental and theoretical dipole moment for ketene and thioketene, it seems that the proposed experimental dipole moment (0.9 D) for selenoketene is somewhat too small. The observed trends of the above properties may readily be understood in terms of how substitution affects the relative importance of the two resonance forms of the ketenes (Scheme 1).

Scheme 1

Ketene is more commonly presented as the "neutral" cumulenic form, which is in resonance with the "zwitterionic" form where the C_β atom is partially negatively charged and oxygen is partially positively charged. The importance of the zwitterionic resonance hybrid depends on the influence of the X atom on the charge separation, and the formation of a C≡X triple bond. Since sulfur and selenium are more electropositive than oxygen, one might expect the positive charge be better accommodated on the heavier elements and the zwitterionic form might become more important in thioketene and selenoketene. On the other hand, the formation of a C≡X triple bond becomes less favourable with larger X down the group due to the less effective overlap of *p* orbitals. Our calculated properties strongly indicate that thioketene and selenoketene are dominated by the neutral cumulenic form, with a significantly smaller contribution of the zwitterionic form. The calculated C=C bond length in $H_2C{=}C{=}X$ increases in the order of Se < S < O. The increase in C=C stretching frequency with substitution confirms an increase in double-bond character along this bond. In addition, the ^{13}C-NMR chemical shift for the C_β has shifted downfield indicating a decrease of negative charge on this carbon. The strongest evidence comes from the decrease in dipole moment upon substitution. A smaller dipole moment along the series indicates a smaller degree of charge separation, despite the charge centers (C_β and X) are being further apart when oxygen is substituted with sulfur or selenium. In summary, thioketene and selenoketene are better represented by the "neutral" cumulenic form.

Table 2. Calculated properties of $H_2C{=}C{=}X$ (X = O, S, and Se), calculated at the G2(MP2) level unless otherwise stated; experimental values, if available, are given in parentheses

Property	X = O	X = S	X = Se
Geometry[a]			
r_{CH} [Å]	1.080 (1.074)	1.084 (1.085)	1.085 (1.091)
r_{CC} [Å]	1.313 (1.314)	1.310 (1.316)	1.309 (1.303)
r_{CX} [Å]	1.161 (1.160)	1.562 (1.556)	1.709 (1.706)
$\angle_{HCH}$ [°]	121.5 (121.6)	119.2 (119.8)	118.8 (119.7)
Vibrational mode [cm^{-1}]:[b]			
sym C–H stretch	3084 (3070)	3047 (3020)	3037 (3032)
C=X stretch	2154 (2153)	826 (850)	673 (662)
HCH bend	1379 (1388)	1346 (1331)	1340 (1335)
C=C stretch	1134 (1116)	1771 (1757)	1745 (1700)
CH_2 wag	568 (587)	685 (701)	708 (737)
CCX bend (out-of-plane)	518 (528)	409 (378)	418
asym CH stretch	3170 (3165)	3119 (3107)	3108 (3063)
CH_2 rock	964 (978)	910 (922)	893
CCX bend (in plane)	423 (439)	351 (340)	352
NMR chemical shift [ppm][c]			
$^{13}C_\alpha$	191.9 (194.0)[d]	243.8 (255.1)[e]	258.4
$^{13}C_\beta$	1.0 (2.5)[d]	49.4 (50.3)[e]	61.0
H	2.0 (2.43)[d]	3.8	4.4
Dipole moment, μ [Debye][a]	1.438 (1.414)	1.063 (1.01)	1.113 (0.90)
Heat of formation [kJ mol^{-1}]			
$\Delta H_{f,0K}$	–49.1	196.4	244.0
$\Delta H_{f,298K}$	–52.4 (–47.7)[f]	193.6	240.3
Ionization energy [eV][f]			
IE_v	9.85 (9.64)	9.02 (8.89)	8.75 (8.72)
IE_a	9.58 (9.62)	8.94 (8.77)	8.74 (8.7)
Proton affinity [kJ mol^{-1}][f]			
PA_{298K}	819.4 (825.3)	843.3 (826.2)	844.7
Electron affinity [eV]			
EA_v	–1.49	–0.05	0.22
EA_a	–0.39	0.35	0.63

[a] Calculated at the QCISD/6-311+G(2df,p) level. Experimental value taken from ref.[4] – [b] B3-LYP/6-31G(d) values, scaled by 0.9613.[15] Experimental value taken from refs.[5,7] – [c] MP2/6-311G(d,p) values based on the QCISD/6-31G(d) geometry. – [d] Experimental values taken from ref.[1] – [e] The present estimate of the experimental value is obtained by assuming that substituent effect on NMR shift is the same for ketene and thioketene. Experimental NMR shifts are taken from refs.[1,8] – [f] Experimental values taken from ref.[22]

We have examined the charge distribution of the three ketenes using the atoms in molecules (AIM)[18] and natural bond orbital (NBO)[19] approaches. Both methods yield quite different results (Table 3). The NBO analysis leads to a strong negative charge at the C_β atom, consistent with the experimental NMR data. In sharp contrast, the AIM method predicts a strong negative charge at the C_α atom for thioketene and selenoketene. It thus appears that the NBO approach provides a more realistic charge distribution of the ketenes. It is also worth noting that the NBO charges of the C_β atom of the three ketenes correlate well with the observed trend of the ^{13}C-NMR chemical shifts. We have calculated the covalent bond orders based on a partition scheme proposed by Cioslowski and Mixon.[20] Consistent with the calculated geometries, vibrational frequencies, and dipole moments, there is a significant increase in the double bond character of the CC and CX bonds on heavy atom substitution. Therefore, thioketene and selenoketene are best described by the neutral cumulenic structure ($H_2C{=}C{=}X$) with a relatively smaller contribution of the zwitterionic resonance form.

Table 3. Calculated charge distributions and covalent bond orders of $H_2C{=}C{=}X$ (X = O, S, and Se) [MP2/6-311++G(d,p) wavefunction, based on QCISD/6-311+G(2df,p) geometry]

Property	X = O	X = S	X = Se
Atomic charge[a]			
C_α	0.673 (0.814)	–0.088 (–0.839)	–0.167 (–0.562)
C_β	–0.772 (0.069)	–0.599 (0.045)	–0.581 (0.033)
X	–0.396 (–1.077)	0.211 (0.618)	0.270 (0.347)
H	0.248 (0.097)	0.238 (0.088)	0.239 (0.091)
Bond order			
CC	1.728	1.878	1.889
CX	1.499	2.146	2.103
CH	0.927	0.928	0.927

[a] NBO values, with AIM values in parentheses.

With regards to the thermochemical properties of the ketenes, the calculated heat of formation of –52.4 kJ mol^{-1} for ketene, using the atomization approach,[21] is in good agreement with the accepted experimental value of –47.7 kJ mol^{-1}.[22] No experimental heats of formation have been

reported for thioketene and selenoketene. Our predicted G2(MP2) heats of formation (298 K) for thioketene and selenoketene are 193.6 and 240.3 kJ mol^{-1}, respectively. We also note that the heats of formation (298 K) calculated using the computationally more expensive Gaussian-3 (G3)[23] theory for ketene and thioketene are –50.8 and 192.8 kJ mol^{-1}, respectively. Both values are in excellent agreement with the G2(MP2) values, suggesting that the energetics of the ketenes and related systems are sufficiently well treated at this level of theory.

The ionization energies (*IE*) of all three ketenes have been measured experimentally.[22] Our calculated *IE*s are in good overall agreement with experimental values (Table 2) which decreases with heavy atom substitution. As expected, the vertical *IE* (IE_v) is always larger than the corresponding adiabatic value (IE_a). With the substitution of heavier element, the differences between the IE_a and IE_v are smaller. In the case of selenoketene, the two values are virtually identical, suggesting that ionization of this species does not have major effect on the geometry. We would like to note in passing that the inclusion of core electrons in the correlation treatment in general leads to an increase in *IE* of less than 2 kJ mol^{-1} (0.02 eV), and the largest difference of 6 kJ mol^{-1} (0.06 eV) is observed for the adiabatic *IE* of selenoketene. Hence, it appears that for the calculation of ionization energies, the frozen core approximation is adequate.

Ionization of ketenes lead to lengthening of r_{CH} and r_{CC}, a shortening of r_{CX}, and a widening of the $\angle_{HCH}$ (Figure 1). In the case of ketene [at the MP2(FU)/6-31G(d) level], the changes are most noticeable (0.007, 0.087, –0.05 Å for the CH, CC, and CX bond; and an increase of 2.8° for the HCH angle). For selenoketene, only the contraction of the CX bond (by 0.05 Å) is obvious. One can understand these changes in terms of the molecular orbitals of the ketenes, which are schematically presented in Figure 2. Removable of an electron from the highest-occupied molecular orbital (HOMO) (of B_1 symmetry) of the neutral ketene, results in a radical cation of $^2B_1$ electronic state. The HOMO is perpendicular to the plane of the ketene molecule, and can be described as CC bonding and CX antibonding. Thus, removing this electron will weaken the CC but strengthen the CX bond. Compared to oxygen, sulfur and selenium do not overlap as well with C_α. In addition, the coefficient of the X atom in the HOMO increases down the group, while the coefficients of the two carbons decrease. As a result, ionization of thioketene and selenoketene would only have a significant effect on the CX bond.

Experimentally, the gas-phase proton affinities (PA) of ketene and thioketene are available.[22] Here, we note that our calculated PAs are in good agreement with the available experimental values. Further discussion on proton affinity will be given in the Reactivities section below.

The electron affinity (EA) of these species has not been reported. The C_{2v} structure of the ketene radical anion is a transition structure on the MP2/6-31G(d) potential energy surface. The true minimum has C_s symmetry ($^2A'$) where all atoms lie on the same plane except that the $\angle_{CCX}$ shows major deviation from linearity. While capturing an electron

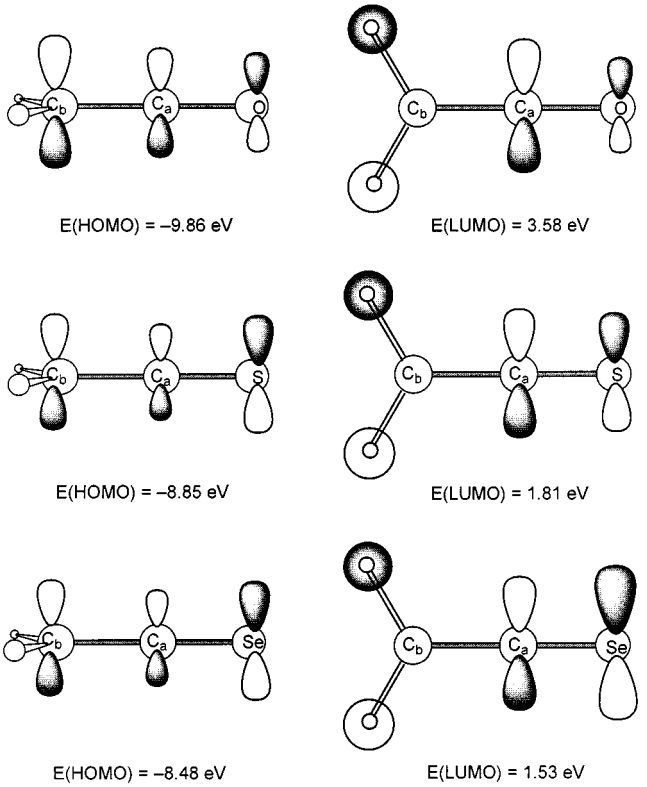

Figure 2. HOMO and LUMO of ketene, thioketene, and selenoketene; the energies of the molecular orbitals are calculated at the MP2(FU)/6-31G(d) level of theory

is a thermodynamically unfavorable process for ketene, substitution of oxygen by sulfur and selenium has transformed this into a favorable process.

Upon addition of an electron, the CX bond length in ketenes increases by 0.074, 0.097, and 0.103 Å, for X = O, S, and Se, respectively, compared to the corresponding neutral ketenes at the MP2(FU)/6-31G(d) level (Figure 1). This trend can be understood in terms of the LUMO of ketene (Figure 2). The LUMO (B_2 symmetry) is on the plane of ketene, again antibonding between C_α and O, with virtually no contribution from the atomic orbitals of C_β. With this antibonding character, the r_{CX} would be longer in the ketene anion than in the neutral. Moreover, for ketene, the AO coefficient on C_α is the largest. Hence, addition of electron will affect the geometry on this atom the most. As in the case of HOMO, the coefficient of the X atom in the LUMO increases down the group while the coefficient of the C_α decreases. Therefore, one would expect the deviation of $\angle_{CCX}$ from linearity to decrease upon substitution. For X = O, S, and Se, the $\angle_{CCX}$ increases from 135.7° to 144.2° to 144.9°, which is in agreement with our qualitative reasoning.

In summary, our calculated properties are in good qualitative agreement with available experimental data. While certain properties such as dipole moments are very sensitive to theoretical model employed, other calculated properties are in quantitative agreement with available experimental

values. This lends strong confidence to the reliability of the reported reactivities below.

Reactivities of Ketene, Thioketene, and Selenoketene

The intrinsic reactivity of the three ketenes are governed by the energies of the frontier orbitals. On heavy atom substitution, the HOMO energy increases while the LUMO energy decreases. This suggests that thioketene and selenoketene would be even more reactive than ketene, which is consistent with the general experimental findings. We also note that while the HOMO–LUMO gap is much larger for ketene, it is quite similar for thioketene and selenoketene. Hence, the reactivity of selenoketene would be quite comparable to that of thioketene in general. To gain insight into the relative reactivity of these ketene systems, we have examined four prototype reactions: ketene-ynol rearrangement, electrophilic, and nucleophilic addition, and [2+2] cycloaddition.

A. Ketene-Ynol Rearrangement: Synthetically, ynols (RC≡COH) are one of the precursors in the preparation of ketenes, and they are interesting species in their own right.[1,24] What would be the effect of sulfur and selenium substitution on the ketene-ynol rearrangement?

Figure 3 displays the schematic potential energy diagram for the rearrangement of ketene (**1**) to ynol (**2**). For all the three ketenes, the corresponding ynol form is always less stable compared to the ketene. However, the relative ynol-ketene energy decreases significantly upon heavy atom substitution.

The rearrangement from **1** to **2** may occur through two plausible pathways: a direct 1,3-hydrogen shift, or two successive 1,2- and 2,3-hydrogen shifts. The two-step pathway occurs via a carbenic intermediate **4** and two transition states (TS **3** and **5**) (Figure 3). For ketene (X = O), we have located all these structures on the pure singlet RHF/6-31G(d) surface, similar to those reported previously at the RHF/4-31G level.[25] However, we have not been able to locate the corresponding structures for **S4** and **Se4** on the RHF/6-31G(d) surface. More importantly, upon the incorporation of electron correlation at the RMP2 level, we failed to locate any stable singlet carbenic structure (**4**), regardless of the nature of X.

On the other hand, we have located a stable equilibrium structure of **4** on both the UHF and UMP2 potential energy surfaces. Interestingly, for **O4**, while RHF yields a non-planar structure, the UHF structure is planar, which reverts to non-planar at the UMP2/6-31G(d) level. Furthermore, we note here that the $<S^2>$ value of structure **4** range from 0.75 to 1.3 for X = O, S, and Se, suggesting that they are of substantial diradical character. Similar diradical character is found for TS **5**. For TS **3**, the diradical character for X = S and Se appears to be minimal as the UHF structure has an $<S^2>$ of less than 0.1. Further optimization of **S3** and **Se3** at the UMP2/6-31G(d) level lead to a final optimized structure that was pure singlet in nature ($<S^2> = 0$).

Given that most of these species are highly spin contaminated, calculations based on the unrestricted Møller–Plesset theory may not yield accurate quantitative energetic information. Instead of using the UMP2 electronic energies in the G2(MP2) protocol, we have used the projected MP2 (PMP2) [26] energies instead. Our modified procedure leads to slightly lower energies (by 1–6 kJ mol^{-1}) for structures **3**, **4**, and **5**. Nevertheless, our current model should be sufficient in providing a qualitative description of the successive hydrogen pathway. Our key finding is that the barrier to rearrangement from carbene **4** to ketene (via TS **3**), and ynol (via TS **5**) appears to be minimal. It is worth noting that the ketene-ynol rearrangement may proceed partly on

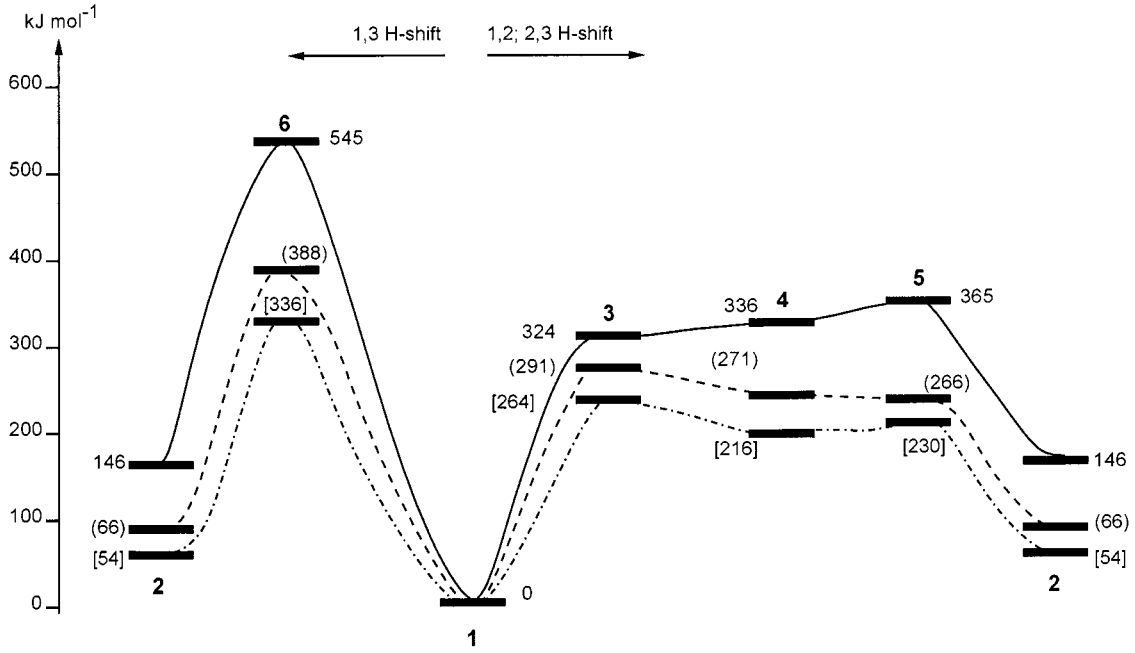

Figure 3. Schematic potential energy surfaces for ketene–ynol rearrangements (solid line for ketene, dashed line for thioketene, and dashed-dotted line for selenoketene); relative energies [G2(MP2)] are in kJ mol^{-1}

the triplet surface. In particular, we found that the triplet carbene is significantly more stable than the singlet state, by 21, 86, and 74 kJ mol^{-1}, for X = O, S, and Se, respectively. Further study using a multi-configuration treatment is in progress.

Direct 1,3-hydrogen shift from **1** to **2** occurs via TS **6** (Figure 3). As this transition structure is highly strained, it is not surprising that the 1,3-hydrogen shift pathway is of higher energy than the two-step pathway. With heavy atom substitution, the ring strain in TS **6** is somewhat relieved, and hence the direct pathway becomes more competitive. To conclude, our calculations indicate that the ketene-ynol rearrangement is both kinetic and thermodynamically favored upon substitution.

Compared to ethenol ($H_2C{=}COH$), ethynol ($HC{\equiv}COH$) is very acidic. In order the understand the origin of the acidity, we carried out bond stabilization energy analysis (Table 4). First we note that all the calculated bond stabilization energies are in good agreement with available experimental data, except for the two reactions involving ethynol (**O2**). While the experimental acidity of ethynol is too high by 57 kJ mol^{-1}, the reaction enthalpy with methane is too high by 49 kJ mol^{-1}. These discrepancies arise from the fact that our calculated $\Delta H_{f,298\,K}$ for ethynol is 94 kJ mol^{-1}, which is significantly different from the reported experimental value of 41.6 kJ mol^{-1}.[22] Given the good agreement between our G2(MP2) and experimental energetics, it is likely that the experimental heat of formation for ethynol is too low. For ethynthiol and ethynselenol, no experimental heat of formation is available, even though the acidity of ethynthiol is reported. Again, the experimental value appears to be too high. Based on our theoretical results here, we would recommend the $\Delta H_{f,298\,K}$ of ethynthiol and ethynselenol to be 261 and 295 kJ mol^{-1}, respectively.

Table 4. Acidities of $H_2C{=}CHXH$ and $HC{\equiv}CXH$ (X = O, S and Se) and bond stabilization energy analysis for enolate, ynolate, enols, and ynols [with the corresponding sulfur and selenium analogs; calculated at the G2(MP2) level]; experimental values, if available, are included in parentheses (derived from experimental enthalpy of formation[22] at 298 K)

Reaction	X = O	X = S	X = Se
[1] $H_2C{=}CHXH \rightarrow H_2C{=}CHX^- + H^+$	1486 (1499)	1441 (1427)	1415
[2] $HC{\equiv}CXH \rightarrow HC{\equiv}CX^- + H^+$	1386 (1443)	1383	1365
[3] $H_2C{=}CHX^- + CH_4 \rightarrow H_2C{=}CH_2 + H_3CX^-$	160 (153)	82	62
[4] $HC{\equiv}CX^- + CH_4 \rightarrow HC{\equiv}CH + H_3CX^-$	220 (214)	138	109
[5] $H_2C{=}CHXH + CH_4 \rightarrow H_2C{=}CH_2 + H_3CXH$	49 (54)	28	20
[6] $HC{\equiv}CXH + CH_4 \rightarrow HC{\equiv}CH + H_3CXH$	10 (59)	26	17

Previously, the very high acidity of ynol, compared to enol, has been attributed to the combination of two effects: stabilization of the ynolate ion, and destabilization of the neutral ynol.[27] However, this difference in acidity between enol (reaction 1) and ynol (reaction 2) decreases from 100 kJ mol^{-1} for X = O to 58 and 50 kJ mol^{-1}, for X = S and Se, respectively (Table 4). With heavy atom substitution, the stability of the "ynolate" anion (reaction 4) decreases slightly compared to the "enolate" anion (reaction 3) from 60 to 56 to 47 kJ mol^{-1} for X = O, S, and Se, respectively. On the other hand, the hydroxyl group is particularly destabilizing in ynol as compared to the substituted analogs (reactions 5 and 6). In the case of X = O, the relative destabilization is 39 kJ mol^{-1}, compared to 2 and 3 kJ mol^{-1} for X= S and Se, respectively. This is probably due to the strong σ-electron withdrawal effect of the highly electronegative oxygen as compared to sulfur and selenium.

Another important isomer of ketene, which is not involved in the ketene-ynol rearrangement, is oxirene (**7**). The nature of this species has attracted a lot of attention.[28,29] It has been found that the lowest-energy vibrational mode, which corresponds to the opening of the three-membered ring, is extremely sensitive to the theoretical model employed. In agreement with previous findings, we found that the symmetric C_{2v} species is a true minimum at HF/6-31G(d) but has a very small imaginary frequency (40 cm^{-1}) at MP2(FU)/6-31G(d). Following the eigenvector of this mode leads us to a structure of C_s symmetry, where the two sets of C–O differ by 0.06 Å, even though the electronic energy is virtually identical to that with the C_{2v} symmetry. This confirms that the ring-opening mode is very soft for ketene, and is sensitive to the effects of electron correlation and basis set. Based on calculation with a highly correlated method and a large basis set [CCSD(T)/TZ2P(f,d)], Vacek concluded that oxirene is a true minimum.

Much less is known about the sulfur and selenium analogs of oxirene (**O7**), namely thiirene (**S7**) and selenoiriene (**Se7**), respectively.[30,31] We have carried out a systematic study on how the frequency of the ring-opening mode is affected by various levels of theory and found that the sensitivity observed in oxirene is not found for thiirene and selenoirene. For example, at the QCISD/6-31G(d) level, this vibrational mode is 117, 469, and 423 cm^{-1} for X = O, S, and Se, respectively. Hence, one can conclude that thioketene and selenoketene are true minima on the C_2H_2X potential energy surface. To facilitate future experimental characterization, the calculated QCISD/6-31G(d) frequencies for **S7** and **Se7** are reported in Table 5.

B. Electrophilic Addition of Ketene: Here, proton is considered as a prototype electrophile. The addition of proton can occur at three different positions: C_α, C_β, and X. The calculated gas-phase proton affinities (0 K) at various sites are summarized in Table 6. For ketene, our calculated proton affinity (820 kJ mol^{-1})[32] is in excellent agreement with the experimental value of 821 kJ mol^{-1}.

Our calculations on the parent ketene suggest that protonation at C_β, resulting in **O8** (acylium ion), is most favorable. Protonation at oxygen yields a stable minimum (**O9**), 178 kJ mol^{-1} higher in energy than **O8**. However, protonation at C_α leads to a transition structure which interconverts **O9** to **O10**. The structure **O10**, 231 kJ mol^{-1}

Table 5. Harmonic vibrational frequencies [cm^{-1}] and infrared intensities [km mol^{-1}] of oxirene, thiirene, and selenoirene [calculated at the QCISD/6-31G(d) level, scaled by 0.9537;[14] intensity values are given in parentheses]

Vibrational Mode	Symmetry	Oxirene	Thiirene	Selenoirene
CH sym rock	a_1	849 (42.7)	661 (8.0)	499 (4.7)
CX str	a_1	1046 (3.8)	897 (1.2)	860 (7.3)
CC str	a_1	1734 (0.7)	1668 (18.0)	1649 (24.2)
CH sym str	a_1	3274 (1.6)	3225 (4.7)	3216 (5.3)
CH asym wag	b_1	471 (80.0)	533 (85.0)	583 (82.3)
CH sym wag	a_2	439 (0.0)	669 (0.0)	700 (0.0)
ring deformation	b_2	117 (0.5)	469 (0.8)	423 (0.4)
CH asym rock	b_2	904 (6.5)	921 (45.1)	887 (67.6)
CH asym str	b_2	3208 (31.5)	3175 (16.0)	3168 (16.4)

Table 6. Proton affinities (0 K) of $H_2C{=}C{=}X$ (X = O, S, and Se) at various possible sites of protonation, calculated at the G2(MP2) level

Site of protonation	X = O	X = S	X = Se
C_α	589.1	726.9	754.5
X	641.9	734.9	748.0
C_β	820.3	843.5	844.8

less stable than **O8**, can be described as a minimum with a the oxygen bridging between C_α and C_β. All these results are in agreement with previous theoretical findings.[33,34]

The relative stabilities of various protonated thioketene structures have been studied at the HF level of theory [35] but we are not aware of any corresponding study for selenoketene. As with ketene, protonation at C_β is still most preferred for thioketene and selenoketene. However, they differ from ketene in three aspects. Firstly, on the HF potential energy surface for the protonated thioketene and selenoketene, four minima are found. Apart from the three analogous minima on the protonated ketene surface, the transition structure which corresponds to protonation at C_α is now a minimum. Nevertheless, this structure is much higher in energy (by at least 80 kJ mol^{-1}) than the other minima. Moreover, this minimum becomes a transition structure at the correlated level [MP2(FU)/6-31G(d)], suggesting that protonation at the C_α may not be stable. Secondly, protonation at sites other than at C_β has become more competitive, and lastly, while protonation at oxygen is clearly favored over the bridged structure, this preference is less obvious for thioketene and selenoketene. In fact, for selenoketene, the Se-bridged structure is slightly preferred (by 7 kJ mol^{-1}) over Se-protonated form.

The preference for the site of protonation in these ketene systems can be explained by a combination of molecular orbital and electrostatic arguments. For the ketene HOMO, the largest orbital coefficient occurs at the valence *p* orbital of C_β. In addition, this carbon atom is negatively charged, as suggested by the NBO analysis (Table 3). Hence, both factors suggest that protonation at this atom would be preferred. With substitution by a heavier atom, the coefficient of this valence atomic orbital decreases and hence the other protonation sites become more competitive. If this factor alone is considered, then the protonation at S or Se (**9**), would be more favored over the bridged structure (**10**). Nevertheless, the charge on S or Se remains positive (Table 3), and hence, protonation on these sites are electrostatically not favorable. As mentioned in the previous section, the C_β atom in selenoketene is more negative than that in thioketene. Apparently, it is this electrostatic attraction that helps to stabilize structure **Se10** over **Se9**.

The preference of protonation at C_β may also be attributed to the fact that the acylium ion is stabilized by the resonance structure $CH_3C{\equiv}X^+$ (Scheme 2).

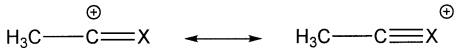

Scheme 2

Sulfur and selenium have a better ability to accommodate positive charge. Thus, proton affinities of thioketene and selenoketene are higher than the parent ketene.

C. Nucleophilic Addition of Ketene: The susceptibility to nucleophilic attack is one of the most characteristic properties of ketenes. The hydration of ketene is considered as a prototype nucleophilic addition reaction here. The addition of water to ketene may yield two products: addition to the C=C bond gives acetic acid while addition to the C=O bond yields enediol. The two competitive processes have been studied, both experimentally[36] and theoretically.[37–39] In a theoretical study by Skancke,[39] the effect of how the actual number of water molecules participating in the reaction affects the potential energy surface was investigated. He concluded that even though the 1-ketene:1-water potential energy surface is quantitatively different from that of a 1-ketene:2-water surface, similar qualitative conclusion could be drawn: the formation of acetic acid is the thermodynamically favored product, while enediol is slightly favored kinetically.

Here we studied the reaction of ketene, thioketene, and selenoketene with a single water molecule. The schematic potential energy surfaces are presented in Figure 4. For ketene, the surface obtained at the G2(MP2) level is very similar to that obtained previously.[39] The hydration process is initiated when a water molecule weakly coordinates itself onto the ketene to form a van der Waal complex (**11**, which is omitted in Figure 4 for simplicity). The formation of acetic acid (**12**) occurs via a four-centered transition structure **13**, while enediol (**14**) is formed via transition structure **15**.

Substitution with a heavy atom does not change the qualitative conclusion for the thermodynamically preferred product (**12**). However, kinetically, the formation of the acid becomes much less competitive: the energy difference between the two transition states (**13** and **15**) is 11 kJ mol^{-1} for ketene, increasing significantly to 87 and 109 kJ mol^{-1}, for thioketene and selenoketene, respectively. This suggests that the hydration of thioketene and selenoketene should yield the corresponding enediols if the reaction is kinetically controlled.

Unlike the ketene-ethene [2+2] cycloaddition reaction discuss in next section, both the HOMO and LUMO of

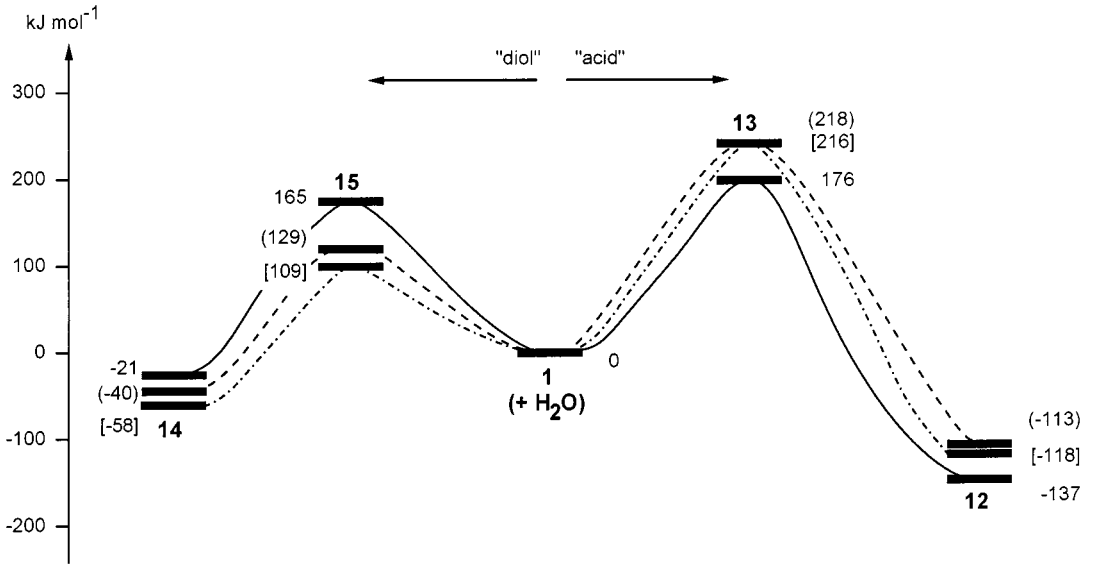

Figure 4. Schematic potential energy surfaces for hydration reaction of ketenes (solid line for ketene, dashed line for thioketene, and dashed-dotted line for selenoketene); relative energies [G2(MP2)] are in kJ mol^{-1}

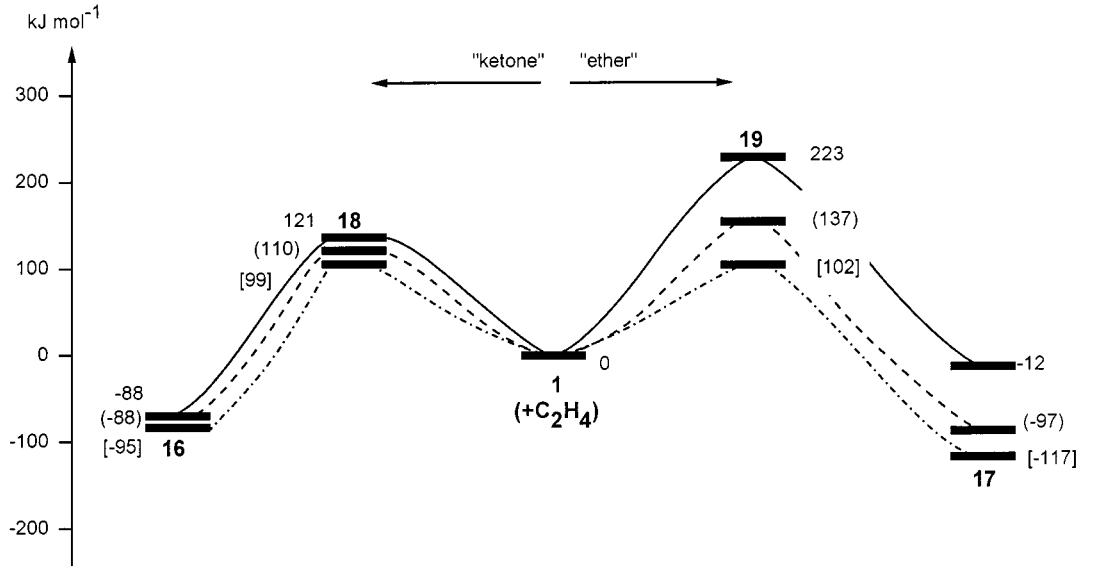

Figure 5. Schematic potential energy surfaces for [2+2] ketene–ethene cycloadditions (solid line for ketene, dashed line for thioketene, and dashed-dotted line for selenoketene); relative energies [G2(MP2)] are in kJ mol^{-1}

water are of the correct symmetry to interact with the frontier orbitals of ketene. The HOMO(ketene)–LUMO(water) gap is about 1.6 eV (calculated at MP2(FU)/6-31G(d) level) higher than the HOMO(water)–LUMO(ketene) gap. Hence, the later pair of interaction would be stronger. This explains why **O15** is more stable than **O13**, and enediol is the preferred hydration product.

Formation of acid (**12**) occurs, via transition structure **13**, when the LUMO (which lies in the molecular plane) of water molecule interacts with the ketene HOMO which is perpendicular to the ketene plane. The coefficients of the two carbons decrease with heavy atom substitution, which explains the higher barrier for acid formation. On the other hand, formation of enediol (**14**) occurs via a four-centered transition structure (**15**), where C_α and X on the ketene are involved. The water molecule directs its lone pair in the HOMO (which is perpendicular to the molecular plane) to interact with the LUMO of the ketene. The coefficient of X increases with heavy atom substitution, suggesting a more favorable interaction.

D. [2+2] Ketene–Ethene Cycloaddition: The [2+2] cycloaddition of ketene with alkene occupies a central role in the understanding of reaction theory and it has been the subject of numerous experimental and theoretical studies.[1,40,41] Two modes of addition are possible: CC addition leads to a cyclic ketone (**16**) while CO addition gives a cyclic ether (**17**). Both reactions are symmetry allowed, which involve the interaction of the frontier orbitals of ketene and ethene in two different fashions. To date, many studies suggest that the [2+2] cycloaddition reaction could proceed by a concerted route, or via the formation of a zwitterion intermediate. The route taken is highly dependent on the nature

of ketene and alkene involved. It is believed that, for the parent ketene and ethene, the concerted route is preferred. We have attempted to locate a zwitterionic minimum on the potential energy surface at HF, B3-LYP, and MP2 level of theory with the 6-31G(d) basis for X = S and Se. All such attempts failed as the species invariably dissociated into ketenes and ethene. This suggests that for thioketene and selenoketene, as in the case of ketene, the reaction is unlikely to proceed by a zwitterionic pathway. This is understandable as the zwitterionic route will involve a negatively charged X. With the decrease of electronegativity down a group, if the ketene-ethene cycloaddition does not go through the zwitterionic route, it would be even less likely that thioketene and selenoketene will.

We have examined the concerted pathway of both CC and CO addition using the G2(MP2) theory (Figure 5). For CC addition, the transition structure involved (**18**) is highly asynchronous, where the difference of the two sets of CC bond lengths is approximately 0.66 Å, virtually independent on the nature of the ketene. Wang and Houk described this type of reaction as a [2+2+2] reaction.[41] Likewise, the transition structure for CO addition (**19**) involves ethene interacting with C_α and X, has a significantly shorter CC bond than the CO bond. Upon substitution on the ketene, the HOMO becomes higher-lying, while the LUMO becomes more low-lying. Thus, both HOMO(ethene)–LUMO(ketene) and HOMO(ketene)–LUMO(ethene) gaps decrease with heavy atom substitution. As a consequence, lower reaction barriers are predicted for both cycloaddition pathways.

For ketene, formation of cyclobutanone is thermodynamically favored over the cyclic ether. However, relative stability of the two addition products is reversed for thioketene and selenoketene. One can explain this trend of stability in terms of the degree of strain in the products. The formation of cyclic ketone (**16**) is not favorable as the product is highly strained. However, upon substitution, the ring strain in cyclic ether (**17**) is somewhat relieved, which is reflected in the increase of the calculated CCC angle of **17** (Figure 1).

Kinetically, both the CC and CO addition pathways become more competitive upon substitution. In fact, the calculated barriers for the formation of both products involving selenoketene are identical. The lowering of barrier in the selenoketene case is partly due to the stabilization of the cyclic ether, in accordance with the Hammond principle. Moreover, the barrier is lowered because of the favorable overlap of the frontier molecular orbitals involved. On going from O to S and to Se, the orbital coefficient of X increases in the HOMO while the coefficient of C_α decreases. All these factors suggest that the reaction between selenoketene and ethene will yield a cyclic ether (**Se17**), rather than a cyclic ketone (**Se16**).

Conclusions

We have examined the properties and reactivities of ketene, thioketene, and selenoketene using ab initio calculations. Calculated structures, vibrational frequencies, dipole moments, NMR chemical shifts, and charge distributions strongly suggest that thioketene and selenoketene are best represented by the neutral cumulenic form. For all prototype reactions studied, thioketene and selenoketene are found to be more reactive than ketene. In terms of chemistry, thioketene resembles selenoketene more than ketene. The variation of reactivity can be readily explained in terms of strain energy, electronegativity, and molecular orbital arguments.

Acknowledgments

M. W. W. thanks the National University of Singapore for financial support (grant no: 970620).

[1] T. T. Tidwell, *Ketenes*, Wiley, New York, **1995**.
[2] A. Wendel, *Selenium in biology and medicine*, Springer-Verlag, Berlin, **1988**.
[3] W. Dekant, G. Urban, C. Gorsmann, M. W. Anders, *J. Am. Chem. Soc.* **1991**, *113*, 5120–5122.
[4] J. Leszczynski, J. S. Kwiatkowski, *Chem. Phys. Lett.* **1993**, *201*, 79–83.
[5] J. L. Laboy, D. J. Clouthier, *Chem. Phys. Lett.* **1995**, *236*, 211–216.
[6] P. Metzner, A. Thuillier, *Sulfur reagents in organic synthesis*, Academic-Press, London, **1994**.
[7] D. J. Clouthier, D. C. Moule, *Top. Curr. Chem.* **1989**, *150*, 167–247.
[8] E. Schaumann, *Tetrahedron* **1988**, *44*, 1827–1871.
[9] M. J. Frisch, G. W. Trucks, H. B. Schlegel, P. M. W. Gill, B. G. Johnson, M. A. Robb, J. R. Cheeseman, T. Keith, G. A. Petersson, J. A. Montgomery, K. Raghavachari, M. A. Al-Laham, V. G. Zakrzewski, J. V. Ortiz, J. B. Foresman, C. Y. Peng, P. Y. Ayala, W. Chen, M. W. Wong, J. L. Andres, E. S. Replogle, R. Gomperts, R. L. Martin, D. J. Fox, J. S. Binkley, D. J. Defrees, J. Baker, J. P. Stewart, M. Head-Gordon, C. Gonzalez, J. A. Pople, *Gaussian 94, Revision D.3*, Gaussian, Inc., Pittsburgh, PA, **1995**.
[10] M. J. Frisch, G. W. Trucks, H. B. Schlegel, G. E. Scuseria, M. A. Robb, J. R. Cheeseman, V. G. Zakrzewski, J. A. Montgomery, Jr., R. E. Stratmann, J. C. Burant, S. Dapprich, J. M. Millam, A. D. Daniels, K. N. Kudin, M. C. Strain, O. Farkas, J. Tomasi, V. Barone, M. Cossi, R. Cammi, B. Mennucci, C. Pomelli, C. Adamo, S. Clifford, J. Ochterski, G. A. Petersson, P. Y. Ayala, Q. Cui, K. Morokuma, D. K. Malick, A. D. Rabuck, K. Raghavachari, J. B. Foresman, J. Cioslowski, J. V. Ortiz, B. B. Stefanov, G. Liu, A. Liashenko, P. Piskorz, I. Komaromi, R. Gomperts, R. L. Martin, D. J. Fox, T. Keith, M. A. Al-Laham, C. Y. Peng, A. Nanayakkara, C. Gonzalez, M. Challacombe, P. M. W. Gill, B. Johnson, W. Chen, M. W. Wong, J. L. Andres, C. Gonzalez, M. Head-Gordon, E. S. Replogle, J. A. Pople, *Gaussian 98, Revision A.6*, Gaussian, Inc., Pittsburgh, PA, **1998**.
[11] L. A. Curtiss, K. Raghavachari, J. A. Pople, *J. Chem. Phys.* **1993**, *98*, 1293–1298.
[12] J. Leszczynski, J. S. Kwiatkowski, D. Leszczynska, *J. Am. Chem. Soc.* **1992**, *114*, 10089–10091.
[13] B. J. Duke, L. Radom, *J. Chem. Phys.* **1998**, *109*, 3352–3359.
[14] A. P. Scott, L. Radom, *J. Phys. Chem.* **1996**, *100*, 16502–16513.
[15] M. W. Wong, *Chem. Phys. Lett.* **1996**, *256*, 391–399.
[16] K. Wolinski, J. F. Hinton, P. Pulay, *J. Am. Chem. Soc.* **1990**, *112*, 8251–8260.
[17] B. Bak, O. J. Nielsen, H. Svanholt, A. Holm, *Chem. Phys. Lett.* **1978**, *53*, 374–376.
[18] R. F. W. Bader, *Atoms in Molecules – A Quantum Theory*, Oxford University Press, Oxford, **1990**.
[19] A. E. Reed, L. A. Curtiss, F. Weinhold, *Chem. Rev.* **1988**, *88*, 899–926.
[20] J. Cioslowski, S. T. Mixon, *J. Am. Chem. Soc.* **1991**, *113*, 4142–4145.

[21] A. Nicolaides, A. Rauk, M. N. Glukhovtsev, L. Radom, *J. Phys. Chem.* **1996**, *100*, 17460–17464.
[22] W. G. Mallard, P. J. Linstrom, *NIST Chemistry WebBook, NIST, Standard Reference Database Number 69*, National Institute of Standards and Technology, Gaithersburg, MD 20899 (http://webbook.nist.gov), **1998**.
[23] L. A. Curtiss, K. Raghavachari, P. C. Redfern, V. Rassolov, J. A. Pople, *J. Chem. Phys.* **1998**, *109*, 7764.
[24] A. J. Kresge, *Acc. Chem. Res.* **1990**, *23*, 43–48.
[25] W. J. Bouma, R. N. Nobes, L. Radom, C. E. Woodward, *J. Org. Chem.* **1982**, *47*, 1869–1875.
[26] H. B. Schlegel, *J. Chem. Phys.* **1986**, *84*, 4530.
[27] B. J. Smith, L. Radom, A. J. Kresge, *J. Am. Chem. Soc.* **1989**, *111*, 8297–3299.
[28] A. P. Scott, R. H. Nobes, H. F. Schaefer, III, L. Radom, *J. Am. Chem. Soc.* **1994**, *116*, 10159–10164.
[29] G. Vacek, J. M. Galbraith, Y. Yamaguchi, H. F. Schaefer, III, R. H. Nobes, A. P. Scott, L. Radom, *J. Phys. Chem.* **1994**, *98*, 8660–8665.
[30] P. E. M. Siegbahn, M. Yoshimine, J. Pacansky, *J. Chem. Phys.* **1983**, *78*, 1384–1389.
[31] B. D. Larsen, H. Eggert, N. Harrit, A. Holm, *Acta Chem. Scand.* **1992**, *46*, 482–486.
[32] M. A. Armitage, M. J. Higgins, E. G. Lewars, R. E. March, *J. Am. Chem. Soc*. **1980**, *102*, 5064.
[33] R. H. Nobes, W. J. Bouma, L. Radom, *J. Am. Chem. Soc.* **1983**, *105*, 309–314.
[34] R. Leung-Toung, M. R. Peterson, T. T. Tidwell, I. G. Csizmadia, *J. Mol. Struct. (Theochem)* **1989**, *183*, 319–330.
[35] C. F. Rodriquez, A. C. Hopkinson, *Can. J. Chem.* **1987**, *65*, 1209–1213.
[36] E. Bothe, A. M. Dessouki, D. Schulte-Frohlinde, *J. Phys. Chem*. **1980**, *84*, 3270.
[37] M. A. McAllister, A. J. Kresge, I. G. Csizmadia, *J. Mol. Struct. (Theochem)* **1992**, *258*, 399–400.
[38] B. M. Allen, A. F. Hegarty, P. O'Neill, M. T. Nguyen, *J. Chem. Soc., Perkin Trans. 2* **1992**, 927–934.
[39] P. N. Skancke, *J. Phys. Chem.* **1992**, *96*, 8065–8069.
[40] F. Bernardi, A. Bottoni, M. A. Robb, A. Venturini, *J. Am. Chem. Soc.* **1990**, *112*, 2106–2114.
[41] X. Wang, K. N. Houk, *J. Am. Chem. Soc*. **1990**, *112*, 1754–1756.

Received November 2, 1999
[O99608]